International Multidisciplinary
Research Journal

Golden Research Thoughts

Chief Editor
Dr.Tukaram Narayan Shinde

IMPACT OF ALUMINIUM AND ZINC SUBSTITUTION ON THE STRUCTUREAL AND MAGNETIC PROPERTIES OF SOL-GEL AUTO COMBUSTION DERIVED NANOSIZED Co-Ni-Zn MIXED FERRITES

Vinod Tukaram[1] , Dhanraj. R. mane[2] , Ramkrishna H Kadam[3] and Ankush B Kadam[4]

[1,4] Jawahar Arts, Science and Commerce college, andur, Tuljapur, Osmanabad, Maharashtra-413603
[2] Registrar, Dr. Babasaheb Ambedkar Marathwada University Aurangabad 431004, India.
[3]Srikrishna Mahavidyalaya Gunjoti, Omerga, Osmanabad, Maharashtra 413613, India.

Abstract:- Nano-crystalline ferrites $Co_{0.5}Ni_{0.5-x}ZnxAlyFe_{2-y}O_4$ with stoichiometric proportion (x= 0.0, O . y= .0, 0.2, O . 8e)e synthesized by the Sol-gel auto combustion method. The doping effect of Al-Zn on crystalline phase, particle size, and saturation magnetization (Ms) are investigated. The resultant powders were sintered at 800°C for 4 hours and were characterized by XRD, FTIR and VSM. XRD analysis showed cubic spinel and the crystallite sizes (D) in the range of 46-7nm. The values of lattice parameter (a) and X-ray density (dx), Bulk density (dB), Hopping length at A-site L_A and at B-site L_B, Specific surface area (S) decreased with the increase of Al-Zn content. Porosity (P) increase from 35.87 - 41.81% and The Ms decreases from 41-14emu/g and coercivity decreases with increase in Al-Zn content except for small increase from x= 0.4 and y = 0.8.

Keywords: Ferrite nanoparticles, Structural properties, Magnetic properties.

1.INTRODUCTION

In the recent past the research interests in nano crystalline Ferrites materials have grown considerably increased because of their large novel physical aspects [1]. Ferrites with spinel structure represent the important class of magnetic materials. The combination of structural, magnetic and electrical properties makes ferrite useful in many technological applications. Owing to their numerous applications ferrites are being studied from last six to seven decades with a view to understand and improve their properties for suitable applications. Many efforts have been taken by researchers to study the structural, electrical and magnetic properties of ferrites [2]. One of the important ways of modification of properties of ferrites is dependent on synthesis methods. A number of chemical routes have been used for the synthesis of ferrite nanoparticles and these methods includes micro emulsion [3], chemical co-precipitation [4] etc. Among these methods sol-gel method is widely used for the synthesis of ferrite nanoparticles. The size and the properties of spinel ferrite nanoparticles can be greatly depend on pH, fuel, stirring time and speed, metal nitrates to fuel ratio etc. Many researchers studied the effect of nonmagnetic Al or Zn substitution in the ferrite system such as NiCoMnCu [5], Co- [6], MnZn [7], CoZn [8], and Mg– [9], Ni– [10] and Ni–Mg [11] etc. These studies revealed that though no studies of Al3+-Zn2+ substitution in the Co-Ni- Zn ferrite sol-gel method

In this work, Al-Zn substituted CoNiZn ferrite has been synthesized by the sol–gel auto combustion and to investigate the structural and magnetic properties. From sol-gel Auto-combustion method requires low temperature and less time, produces homogenous particles of uniform size. To our best of knowledge, a systematic investigation of structural and magnetic properties of CoNiZn ferrite nanoparticles prepared by sol-gel auto combustion technique is not presented in the literature. In the present work, we report the structural and magnetic properties of cobalt nickel zinc ferrite ($CoNiZnFe_2O_4$) nanoparticles.

Vinod Tukaram[1] , Dhanraj. R. mane[2] , Ramkrishna H Kadam[3] and Ankush B Kadam[4], "IMPACT OF ALUMINIUM AND ZINC SUBSTITUTION ON THE STRUCTUREAL AND MAGNETIC PROPERTIES OF SOL-GEL AUTO COMBUSTION DERIVED NANOSIZED Co-Ni-Zn MIXED FERRITES ", Golden Research Thoughts | Volume 4 | Issue 7 | Jan 2015 | Online & Print

1

2. EXPERIMENTAL

2.1. Preparation of Al-Zn substituted Co-Ni-Zn ferrites:

In this work sol– gel auto ignition method were used for the preparation of Al-Zn-substituted Co-Ni-Zn ferrites NPs having compositions. $Co_{0.5}Ni_{0.5-x}Zn_xAlyFe_{2-y}O_4$ (x= 0.0, O . 4 and y= 0, 0.2, O . 8) with stoichiometric proportions of AR grade cobalt, nickel, zinc, Aluminium and iron nitrates and citric acid as raw ingredients were dissolved in distilled water to obtain a mixed solution. The molar ratio of metal nitrates to citric acid was 1:3. Adjust the pH=7 in the above solution. The obtained mixed sols were heated at 80 ^oC on a hot plate magneto-stirrer and continuously stirred to transform into a gel. When ignited at any point, the dried gel burned in a self-propagating combustion way until all gels were burned completely out to form loose precursors. Finally, The resultant product powders were obtained after calcining at 800 °C for 4 h [12].

2.2. Instrumentation:

X-ray diffraction patterns of the samples were Conducted on Philips X-ray diffractometer (model 3710; PANalytical B.V., Almelo, The Netherlands) with CuK radiation (= 1 . 5 4 0 5 A°). Mean crystallite sizes of the samples were estimated from broadening of the most intense XRD peaks, using Scherrer's formula $D = 0.9$ / B(cos B) where is X-ray wave length, B is line broadening (just due to crystallite size) and B is the Bragg angle. The magnetic characteristic hysteresis loops of the system were measured at room temperature, up to a maximum external field of +8 kOe, by using a commercial PARC EG&G VSM 4500 vibrating sample magnetometer (Princeton Applied Research Corporation, Oak Ridge, TN, USA). FTIR spectra of all the samples were recorded in KBr medium in the range 400–4000 cm^{-1} with a Thermo Nicolet Nexus FTIR (model 870).

3. RESULTS AND DISCUSSIONS

3.1. XRD Analysis:

X-ray diffraction patterns of Al-Zn substituted $Co_{0.5}Ni_{0.5-x}Zn_xAlyFe_{2-y}O_4$ ferrite Samples (x = 0.0, O . 4 and y = 0.0, 0.2, O . 8) It is observed that all the XRD patterns clearly showed the reflection has 220, 311, 222, 400, 422, 333 and 440 come from plane that indicates formation of single phased cubic spinel structure, with no additional peaks. A closer inspection of the XRD patterns reveals that the peak intensities have becomes broader with an increase of Al^{3+} and Zn^{2+} substitution. This is due to the substitution of Al^{3+} ions in place of Fe^{3+} ions which lowers the crystallite size. The results are shown in Fig-1 and Table-1.

The lattice constant 'a' is determined from the XRD data by using powder-x-software [13] are given in Table 1 shown that In the present series The decrease in lattice constant is attributed to the replacement of Fe^{3+} ions of larger ionic radius (0.64 A°) by smaller Al^{3+} ions (0.50 A°), which causes shrinking in the unit cell dimensions. Similar trend was found in Cu-Cd ferrite with aluminium substitution [14].

Lattice parameter "a" of individual composition was calculated by using the following formula: a=d $(h^2 + k^2 + l^2)$, where a = lattice parameter, d = inter planar distance, hkl = miller indices

The average particle size for each composition has been calculated using the Scherrer formula [15]: D=K / cos . where = Wavelength of X-ray, = Full width and Half Maxima in radians, = Bragg's angle at the peak position. the sizes of crystallites in the sample were evaluated by measuring the FWHM of the most intense peak (311). The results are tabulated in Table 1. Particle size decreases from 46 nm to 7 nm with an increase in nonmagnetic Al-Zn substitution. The same trend in variation of crystallite size was observed in Mn-Zn [16] and Ni–Al ferrite system [17].

The X-ray density of each sample was calculated using the formula [18]: $dx = ZM / Na^3$. where Z = Number of molecules per unit cell (8), M = Molecular weight of the sample, N = Avagadro's Number, a = lattice parameter and the results are shown in Table-1. It is obvious that, the values of X-ray density, for each sample, decreases with increasing Al-Zn content could be attributed to the atomic weight and the radii of constituent ions and hence follows similar trend as that of lattice constant, this is due to the fact that the decrease in mass (due to replacement of greater atomic weight of Fe-55.847 gm/mole by less atomic weight of Al-26.982 gm/mole) over takes the decrease in volume (V) of the unit cell in the system.

Volume of unit cell was calculated by using the formula; $V = a^3$ in $(A^0)^3$, where 'a' is lattice parameter. Volume of unit cell was found to decrease with increase in Al-Zn content, as it depends on lattice parameter which has decreased with increase in Al-Zn content. The calculated values were tabulated in Table 1.

The distance L_A and L_B between the magnetic ions at A-site and B-site respectively can be obtained where, $L_A = 0.25$ a √3, and $L_B = 0.25$ a √2, where 'a' is the lattice parameter [19]. The obtained values of L_A and L_B are listed in Table 1. It is clear that L_A and L_B reflect the same behaviour of a, where they decrease with increasing Al-Zn ion content. This may be due to the shrinking of the unit cell dimensions arising from the substitution of relatively smaller Al^{+3} ions instead of Fe^{+3} ions.

The specific surface area (S) was calculated from the diameter of the particle in nanometers and the measured density in g/cm^3 using the following relation: S =6000/D dB [20], where D is the crystallite size and dB is the bulk density. The specific surface area increases with increasing Al-Zn content. The increase in S is due to the decrease in crystallite size. The values of surface area are given in Table 1.

Bulk density (d_B) measured using the formula: $d_B = m/ \pi r^2 h$ [21], where 'm' is the mass, 'r' is the radius and 'h' is the height of the pellet. Table 1 shows that the bulk density decreases with the increase in Al-Zn content. The decrease in bulk density can be co-related with the decrease in crystallite size. The percentage porosity is calculated using the following relation: P= (1 - d_B/d_x) 100[21], Where d_x and d_B are the X-ray density and bulk density respectively. The values are given in Table 1, shows that the porosity increases with increase in Al-Zn substitution. The increase in porosity is related to decrease in crystallite size and bulk density.
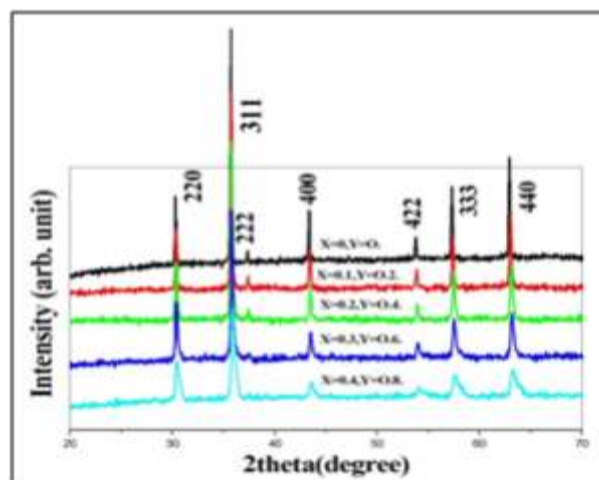

Figure.1 XRD patterns of $Co_{0.5}Ni_{0.5-x}Zn_xAl_yFe_{2-y}O_4$

3.2 FT-IR studies

The FT-IR spectra of the samples in the range; 4000–400 cm^{-1} and the results are tabulated in Fig-2 and Table-1. There can be seen the presence of two main absorbtion peaks. The higher frequency band (ν_1) (583.12-617.29 cm^{-1}) and lower frequency band (ν_2) (434- 498.45 cm^{-1}) are assigned to the tetrahedral and octahedral sites respectively [22, 23]. It explains that the normal mode of vibration of the tetrahedral cluster is higher than that of the octahedral cluster. It should be attributed to the shorter bond length of the tetrahedral cluster and the longer bond length of the octahedral cluster [24]. Hence, vibrational frequency of the first one is larger than the second one (400<600 cm^{-1}). The bonds observed around 3432-3336 and 1632 cm^{-1} frequencies of ascribed due to the tensional stretching modes and H-O-H bending vibration of the free or absorbed water molecules [25]. From the Table 1, it is clear that comparison of the observed vibrational frequencies of all samples indicates an increase of the wave number values for both tetrahedral and octahedral vibrations. Increasing the ν_1 and ν_2 wave numbers with increase in Al^{3+} and Zn^{2+} content can be attributed to elementary cell volume decrease as can be follows similar trend as that of lattice constants.
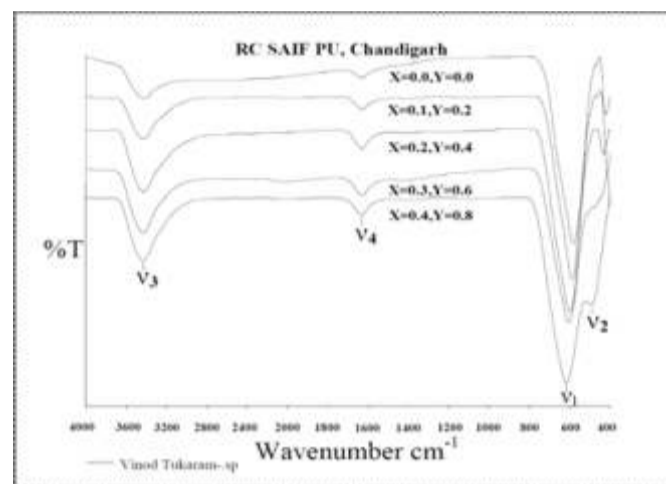
Figure.2 FT-IR patterns of $Co_{0.5}Ni_{0.5-x}Zn_xAl_yFe_{2-y}O_4$

3.3. Magnetic properties

Magnetic hysteresis loops of aluminium and Zinc doped Cobalt nickel Zinc ferrite nanoparticles analyzed using a Magnetometer (VSM) at room temperature. As observed the hysteresis loops become more and more narrow as the Al-Zn content increases. The saturation magnetization (Ms) and coercivity (Hc) values have been directly extracted from these curves. From table 1 show that with increasing Al-Zn content   the magnetization M (at the same outer conditions), remanent magnetization Mr, saturation magnetization Ms, the squareness ratio (Mr/Ms) and coercive field Hc all decrease monotonously. The results are shown in Fig-3 and Table-1.

From Table 1, it is clear that Ms decreased from 41.19 to 14.85 emu/g by doping Co-Ni-Zn ferrite with nonmagnetic Al^{3+} and Zn^{2+} simultaneously, a gradual decrease in saturation magnetization. This decrease in Ms value may be due to the weakening of A-B interaction. In the present case, the concentration of Fe^{3+} ions at the octahedral (B) site decreases due to the replacement of Al^{3+} ions on B-sites, that is, A-B super exchange interaction decreases [26] and hence changing the magnetic structure, resulting in a lowered Ms values because due to the two factors. Firstly, that Al^{3+} ion of low magnetic moment values (0μB) replace Fe^{3+} ions of high magnetic moment (5μB), which results in the dilution of the magnetization at the B-site reducing the B-sublattice magnetization [27]. Secondly, the spin canting introduced by Zn^{2+} at tetrahedral sites.

The value of remnant magnetization Mr and the remnant ratio (Mr/ Ms) obtained for Al-Zn doped cobalt nickel zinc ferrite samples shows a decreasing trend with increasing Al-Zn content (Table 1).

The values of magnetic moment (n_B) for doped Al-Zn ferrites samples are calculated by using the formula n_B =(M_w x Ms)/5585 where M_w is the molecular weight of the composition and M_s is the saturation magnetization[28]. Magnetic moment values were found to decrease with increase in Al-Zn concentration which is attributed to greater occupancy of Al3+ at B sites. The results are tabulated in Table 1.

Hc which is a measure of the magnetic field strength required for overcoming anisotropy to flip the magnetic moments is clearly affected by the Al-Zn substitution. Hc decreased from 1014.88 to 224.48 kOe and then increased x=0.4. y=0.8 in coercivity with increase in Al^{3+} and Zn^{2+} concentrations may be due to the decrease in anisotropy field which in turn decreases the domain wall energy [29]. The increase in coercivity for ferrites with composition x = 0.4. y = 0.8, might be due to the increase in magnetic crystalline anisotropy. The coercivity of the nanoferrites has a contribution from their finite size namely surface anisotropy [30]
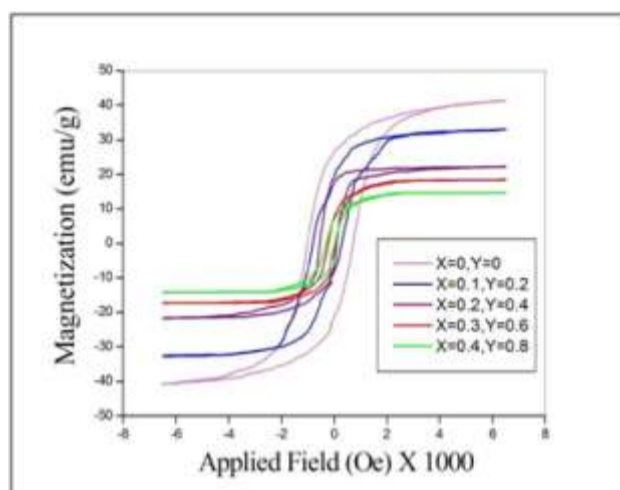
Figure.3 Magnetization curve of $Co_{0.5}Ni_{0.5-x}Zn_xAl_yFe_{2-y}O_4$

Table 1: Lattice constant (a), Particle size (D), X-ray density (dx), bulk density (dB), porosity(P), Volume of unit cell (V), specific surface area (S), hopping length at A-site L_A and at B-site L_B, IR wavenumber ($?_1$ and $?_2$), Saturation magnetization (Ms), manent magnetization (Mr), remanent ratio (Mr/Ms), Coercivity (Hc) and magneton number (nB) of $Co_{0.5}Ni_{0.5-x}Zn_xAl_yFe_{2-y}O_4$.

Samples	X=0,y=0	X=0.1,y=0.2	X=0.2,y=0.4	X=0.3,y=0.6	X=0.4,y=0.8
a (Å)	8.344	8.332	8.327	8.318	8.309
D (nm)	46.72	30.56	23.53	19.85	7.315
$Dx(g/cm^3)$	5.360	5.266	5.159	5.055	4.956
$d_B (g/cm^3)$	3.373	3.367	3.327	3.277	2.883
P(%)	35.87	36.05	37.27	38.16	41.81
V	581.10	578.56	577.40	575.60	573.77
S (m^2/g)	38.06	58.30	76.63	92.21	284.4
LA (Å)	3.613	3.608	3.605	3.601	3.598
LB (Å)	2.950	2.946	2.944	2.941	2.937
$?_1(cm^{-1})$	583.12	588.19	596.21	607.38	617.29
$?_2(cm^{-1})$	-	424.46	427.48	-	498.45
Ms(emu/g)	41.19	33.11	22.21	18.33	14.85
Mr(emu/g)	13.13	8.693	6.735	3.802	3.527
(Mr/Ms)	0.3189	0.3032	0.2625	0.2074	0.2374
Hc(Oe)	1014.8	670.96	439.04	224.48	299.6
$n_B (\mu_B)$	1.729	1.360	0.892	0.756	0.5695

CONCLUSIONS

Nanocrystalline Al-Zn substitution into the Co-Ni-Zn ferrites was successfully prepared using sol–gel auto-combustion technique is a convenient way for obtaining a homogeneous nano sized mixed Co-Ni- Zn ferrites. It is a very simple and economical method. X-ray diffraction pattern confirms the formation of cubic spinel structure and also observed that the lattice constant decreases with increase in Al-Zn substitution. The particle size estimated from Debye-Scherrer's formula varies in the range of 46-7nm. The FTIR spectra show two prominent absorption bands corresponding to the spinel ferrite phase. The decrease of saturation magnetization with increasing Al3+ content occurs because the replacement of Fe^{3+} by Al^{3+} ions weakens the sublattice interaction and lowers the magnetic moments of unit cells. The present study confirms that soft magnetic Co-Ni-Zn nanoferrite materials that were synthesized can be easily magnetized and demagnetized. Such materials are desirable for transformer and motor

cores to minimize the energy dissipation with the alternating fields associated with AC electrical applications.

ACKNOWLEDGEMENTS

REFERENCES

1. M. Zheng, X.C. Wu, B.S. Zhou, Y.J. Wang, J. Magn. Magn.Mater.183 (1998) 152.
2. I. H. Gul, Erum Pervaiz, Mater. Res. Bull. 47 (2012) 1353.
3. H. Nathani, S. Gubbala, and R. D. K. Misra, Materials Science and Engineering B 121   (2005) 126–136.
4. M. R. Anantharaman, S. Jagatheesan, K. A. Malini, S. Sindhu, A. Narayanasamy, C. N. Chinnasamy,   J. P. Jacobs, S. Reijne, K. Seshan, R. H. H. Smits, H.H. Brongersma, Journal of Magnetism and Magnetic Materials 189 (1998) 83-88.
5. T. Ramesh, R. S. Shinde, S. R. Murthy. "Journal of Magnetism and Magnetic Materials" 345(2013), 276–281.
6. R. A. Bugad , T. R. Mane , C. S. Pawar, B. R. Karche. "Golden Research Thoughts" 2 (11) May.2013, ISSN:- 2231-5063.
7. R. L. Dhiman, S. P. Taneja,V. R. Reddy. "Hindawi Publishing Corporation Advances in Condensed Matter Physics" Volume 2008, Article ID 839536, 7 pages doi:10.1155/2008/839536.
8. S T Alone and K. M. Jadhav, Pramana. Journal of physics @ Indian Academy of Sciences Vol. 70, No. 1 January 2008.
9. M. Manjurul Haque, M. Huq, M.A. Hakim, Physica B 404 (2009) 3915.
10. M. Jalaly, M.H. Enayati, P. Kameli, F. Karimzadeh, Physica B 405 (2010) 507.
11. M.A. Amer, M. El Hiti, J. Magn. Magn. Mater. 234 (2001) 118.
12. Shirsath, SE, Kadam, RH, Gaikwad, AS, Ghasemi, A, Morisako, A: Li0.5Fe2.5O4. J. Magn. Magn. Mater. 323(23) (2011) 3104.
13. M. Hashim, Alimuddin, S. Kumar, B. H. Koo, S. E. Shirsath, E. M. Mohammed, J. Shah, R. K. Kotnala, H. K. Choi, H. Chung, J. Alloy. Compd. 518 (2012) 11–18.
14. S. S .Suryawanshi, V .V. Deshpande, U. B. Deshmukh, S. M. Kabur, N. D. Chaudhari, S. R. Sawant, Mat. Chem. Phys. 59 (1999) 199.
15. M. J. Iqbal, S. Farooq, Mater. Sci. Eng., B 136 (2007) 140.
16. E. Auzans, D. Zins, E. Blums, R. Massart, J. Mater. Sci. 34 (1999) 1253.
17. S. M. Patange, et al. Physica B 406(2011)663–668.
18. M. A. Gabal, R. M. ElShishtawy, J. Magn. Magn. Mater. 324 (2012) 2258.
19. M. A. Amer, T. M. Meaz, A. G. Mostafa, M. E. Kastawi, A. I. Ghoneim, Ceram. Int. 40 (2014) 241.
20. C. J. Brinker, G. W. Scherer, Sol-Gel Science: The Physics and Chemistry of Sol-Gel Processing, Academic Press, San Diego, 1990. 527.
21. K. M. Batoo, S. Kumar, C. G. Lee, Alimuddin, Curr. Appl. Phys. 9 (2009) 826.
22. R. D. Waldron, Phys. Rev. 99 (1955) 1727.
23. S. E. Shirsath, S.S. Jadhav, B.G. Toksha, S.M. Patange, K.M. Jadhav, ScriptaMater. 64 (2011) 773.
24. R. Laishram, S. Phanjoubam, H. N. K. Sarma, J. Phys. D: Appl. Phys. 32(1999) 2151
25. I. Sharifi, H. Shokrollahi, J. Magn. Magn. Mater 324 (2012) 2397–2403
26. Gul, IH, Maqsood, A: J. Alloy. Comp. 465, 227–231 (2008)
27. Zhou, B.; Zhang, Y. -W.; Yu, Y. –J.; Liao, C. –S.; Yan, C. –H.; Chen, L.-Y.; Wang, S.-Y. Phys. Rev. B 2003, 68, 24426.
28. J. Smit, H. P. J. Wijn, Philips Technical Library, Eindhoven, Netherlands, 1959.
29. I. H. Gul, Abbasi, A, Amin, F, Anis-ur-Rehman, M, Maqsood, A: J. Magn. Magn. Mater. 311, 494 (2007).
30. S. E. Shirsath, S. S. Jadhav, B. G. Toksha, S. M. Patange, K. M. Jadhav, J. Appl. Phy. 110, 013914 (2011).

Publish Research Article
International Level Multidisciplinary Research Journal
For All Subjects

Dear Sir/Mam,
          We invite unpublished Research Paper,Summary of Research Project,Theses,Books and Book Review for publication,you will be pleased to know that our journals are

Associated and Indexed,India

* International Scientific Journal Consortium
* OPEN J-GATE

Associated and Indexed,USA

* EBSCO
* Index Copernicus
* Publication Index
* Academic Journal Database
* Contemporary Research Index
* Academic Paper Databse
* Digital Journals Database
* Current Index to Scholarly Journals
* Elite Scientific Journal Archive
* Directory Of Academic Resources
* Scholar Journal Index
* Recent Science Index
* Scientific Resources Database
* Directory Of Research Journal Indexing